Bioelectrochemistry 106 (2015) 369–378

Contents lists available at ScienceDirect

Bioelectrochemistry

journal homepage: www.elsevier.com/locate/bioelechem

Cell membrane permeabilization by 12-ns electric pulses: Not a purely dielectric, but a charge-dependent phenomenon

Aude Silve [a,b,c,d,*], Isabelle Leray [b,c,d], Michael Leguèbe [e], Clair Poignard [e], Lluis M. Mir [b,c,d,**]

[a] Institute for Pulsed Power and Microwave Technology, Karlsruhe Institute of Technology, Germany
[b] CNRS, Villejuif, Laboratoire de Vectorologie et Thérapeutiques Anti-cancéreuses, UMR 8203, Villejuif 94805, France
[c] Univ Paris-Sud, Laboratoire de Vectorologie et Thérapeutiques Anti-cancéreuses, UMR 8203, Villejuif 94805, France
[d] Gustave Roussy, Laboratoire de Vectorologie et Thérapeutiques Anti-cancéreuses, UMR 8203, Villejuif 94805, France
[e] Inria Bordeaux, CNRS UMR 5251, Université de Bordeaux, France

ARTICLE INFO

Article history:
Received 30 January 2015
Received in revised form 3 June 2015
Accepted 10 June 2015
Available online 17 June 2015

Keywords:
Medium conductivity
Electroporation
Electropermeabilization
Nanosecond-pulsed electric fields
Temperature

ABSTRACT

Electric pulses of a few nanoseconds in duration can induce reversible permeabilization of cell membrane and cell death. Whether these effects are caused by ionic or purely dielectric phenomena is still discussed. We address this question by studying the impact of conductivity of the pulsing buffer on the effect of pulses of 12 ns and 3.2 MV/m on the DC-3F mammalian cell line. When pulses were applied in a high-conductivity medium (1.5 S/m), cells experienced both reversible electropermeabilization and cell death. On the contrary, no effect was observed in the low-conductivity medium (0.1 S/m). Possible artifacts due to differences in viscosity, temperature increase or electrochemical reactions were excluded. The influence of conductivity reported here suggests that charges still play a role, even for 12-ns pulses. All theoretical models agree with this experimental observation, since all suggest that only high-conductivity medium can induce a transmembrane voltage high enough to induce pore creation, in turn. However, most models fail to describe why pulse accumulation is experimentally required to observe biological effects. They mostly show no increase of permeabilization with accumulation of pulses. Currently, only one model properly describes pulse accumulation by modeling diffusion of the altered membrane regions.

1. Introduction

Electric pulses can induce reversible or irreversible defects in a cell membrane, thus allowing direct access of external molecules to the cell cytosol [1–3]. This effect is referred to as electropermeabilization or electroporation. This technique is nowadays routinely used in research laboratories and clinics e.g. to treat cancerous tissues [4–8]. In traditional electropermeabilization, pulse parameters can be chosen over a wide range and still lead to a successful permeabilization of cells. Values usually range between a few tens or hundreds of μs (pulses which are referred to as micropulses) and a few ms (pulses referred to as millipulses). Field magnitude is chosen depending on the cell type and desired effect, but usually lies between a few tens of kV/m and a few hundreds of kV/m. More recently, different groups found that much shorter and more intense pulses can also lead to a membrane permeabilization [9–13]. Typical electrical parameters mentioned in literature are a few tens of nanoseconds for the duration and at least 2 MV/m for the electric field magnitude. Nomenclature to refer to various types of pulses in literature, however, is not yet homogeneous. Frequently, a distinction is made between 'short pulses' and 'long pulses'. These names usually refer to the charging time of the cell plasma (external) membrane. Indeed, when a cell is subjected to an external field, its plasma membrane charges like a capacitor, with an exponential time course that is characterized by the charging time constant τ. 'Short pulses' and 'long pulses' usually mean pulses shorter and longer than the cell plasma membrane charging time ($\sim 5 * \tau$), respectively. Several electromagnetic models have been developed to precisely describe the behavior of a spherical cell in a homogeneous unidirectional electric field [14–17]. Those models can predict the charging time constant τ of the cell plasma membrane in the linear regime (Eq. (1) [14]). Most of the parameters influencing this charging time constant are intrinsic to the cell and are (almost) inaccessible by the experimental design. This is the case for the cell radius r_c (m), the intracellular conductivity σ_i (S/m), the membrane surface capacitance C_m (F/m^2), and the

* Correspondence to: A. Silve, Institute for Pulsed Power and Microwave Technology, Karlsruhe Institute of Technology, Germany.
** Correspondence to: L.M. Mir, CNRS, Villejuif, Laboratoire de Vectorologie et Thérapeutiques Anti-cancéreuses, UMR 8203, Villejuif 94805, France.
E-mail addresses: aude.silve@kit.edu (A. Silve), luis.mir@gustaveroussy.fr (L.M. Mir).

http://dx.doi.org/10.1016/j.bioelechem.2015.06.002
1567-5394/

membrane surface conductance S_0 (S/m^2). However, the charging time also depends on extracellular conductivity σ_e (S/m), which is a parameter that can be set to different values during an experiment (within the limit of physiologically acceptable values).

$$\tau = r_c C_m \frac{\sigma_i + 2\sigma_e}{2\sigma_e\sigma_i + r(\sigma_i + 2\sigma_e)S_0} \quad (1)$$

The time constant is plotted as a function of the extracellular conductivity in Fig. 1. Other parameters were kept constant and their values are given in the legend of the figure. Values for the time constant range from approximately 93 ns to 420 ns at external conductivities ranging from 1.5 S/m to 0.1 S/m.

Whether the values of Fig. 1 are accurate or not, it can still be assumed that when a cell with a radius of 7 μm is subjected to a 12-ns pulse, its membrane will not reach the stationary value imposed by the pulse, since the charging time is much longer than 12 ns. Moreover, Eq. (1) and Fig. 1 suggest that the charging time of the membrane is highly dependent on the conductivity of the extracellular medium. As a consequence of those two observations, an important influence of extracellular conductivity can be expected. In this study we focused on pulses of 12 ns duration and 3.2 MV/m. In a previous study, it was shown that these types of pulses can induce membrane permeabilization as well as cell death [13]. Here, these effects are shown to correlate with the conductivity of the extracellular medium. We additionally demonstrate that the higher efficiency of the high-conductivity medium is not due to an elevation of temperature.

Experiments were performed on DC-3F cells which grow attached, but can be kept in suspension for the time of the experiments. The cell death caused by the exposure of the cells to the pulses was assessed by cell survival quantified by a cloning efficiency test. Moreover, pulse treatment combined with a nonpermeant cytotoxic agent in the extracellular medium (namely bleomycin [18–22]) provided a robust and quantitative method for determining reversible permeabilization (such a method was already described in [13,23] and the concept of the approach is detailed in [5]).

2. Material and methods

2.1. Cell culture

Chinese hamster lung cell line DC-3F [24] was grown in complete medium, consisting of MEM — Minimum Essential Medium (31095-052, Life Technologies, Saint Aubin, France) with the addition of 10% fetal bovine serum (10270-106, Life Technologies) and supplemented by antibiotics (500 U/ml penicillin and 500 μg/ml streptomycin). Cells were kept in a humidified atmosphere at 37 °C and 5% CO_2 and routinely passed every two days. When they are placed in a suspension, those cells have an average diameter of 13.2 ± 1.3 μm (mean ± standard deviation evaluated from bright light microscopy images; 380 cells were analyzed in five independent experiments).

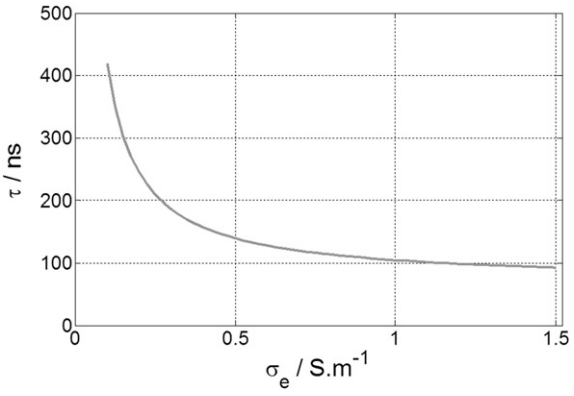

Fig. 1. Charging time as a function of extra-cellular conductivity. The parameters used for the computation are: $r_c = 7$ μm, $\sigma_i = 1$ S/m, $C_m = 0.01$ F/m^2, $S_0 = 1.9$ S/m^2.

2.2. Pulsing media

Two different media were mainly used: Either S-MEM (a Minimum Essential Medium modified for the cultivation of cells in suspension, 11380-037 Life Technologies) or STM (250 mM sucrose, 10 mM Tris HCl pH 7.0, 1 mM $MgCl_2$). Conductivity of the solutions was measured with a *Conductivity Meter CLM 381* (Endress and Hauser, Weil am Rhein, Germany). To measure the dependence of conductivity on temperature, a beaker containing the solution to be tested was heated with a standard heating plate (VHP-C7, VWR International). The two media will hereinafter be referred to as high-conductivity (1.5 S/m) and low-conductivity (0.1 S/m) medium, respectively.

Lyophilized bleomycin was dissolved in S-MEM (or STM) and stored at −20 °C at 300 μM. Aliquots were taken just before the experiments and dissolved in S-MEM (or STM) to obtain media with a concentration of 30 nM of bleomycin. As STM is more viscous than SMEM due to the high concentration of sucrose, "viscous S-MEM" was prepared by adding 0.1% or 0.15% of agar (30391-023, Life Technologies) to the standard S-MEM. These solutions were sterilized by autoclaving prior to the experiments. Viscosity measurements were performed with a viscometer of the type Brookfield DV2T at 24 °C. Results are the mean ± standard deviation of three independent measurements.

2.3. Assessment of cell viability

After trypsinization of exponentially growing cells and inactivation of trypsin (25300-054, Life Technologies) by the serum factors of the complete medium, cells were centrifuged for 10 min at 150 *g* and resuspended at a density of 5×10^6 cells/ml in the appropriate medium containing 30 nM bleomycin or not. Cells were immediately deposited between the two electrodes and exposed to the electric pulses. Cells were kept for 10 min at room temperature after the application of the electric pulses. The cells were then diluted in complete medium. After dilution, cells were seeded in triplicate in complete culture medium (250 cells per cell culture dish, 35 mm in diameter) to measure their viability through a quantitative cloning efficacy test. After 5 days in a humidified, 5% CO_2 atmosphere, colonies were fixed and stained (with a solution of 5% formaldehyde containing crystal violet) and the number of clones N was counted for each condition. Viability was then normalized to the number of clones in the control $N_{control}$ and reported as a percentage of survival: $N/N_{control} \cdot 10^2$. In experiments without bleomycin, the control condition refers to cells subjected to no treatment. In experiments with bleomycin, the control condition refers to cells in contact with the bleomycin, which did not receive any pulses. Viability of unpulsed controls was typically between 90% and 95% after exposure to 30 nM bleomycin. Final results are represented as mean values + SD (standard deviation) of three to five independent experiments.

2.4. Nanosecond-pulse delivery

Unless stated otherwise, a pulse-forming line generator based on spark gap technology and designed by Europulse (Cressensac, France) was used. Cells were exposed in suspension in conventional electroporation cuvettes from Cell project (Harrietsham, United Kingdom). The 4 mm cuvettes were used and precise measurements of the distance between the electrodes indicated $d_{4mm} = 4.19 \pm 0.02$ mm. The measured distance was used to evaluate the electric field inside the cuvette.

During the experiments designed to test the influence of conductivity, special care was taken to impose exactly the same electric field in both the high- and low-conductivity media. To this end, the two cuvettes containing the two different media were exposed in a parallel arrangement as depicted in Fig. 2. This ensures that an identical voltage is

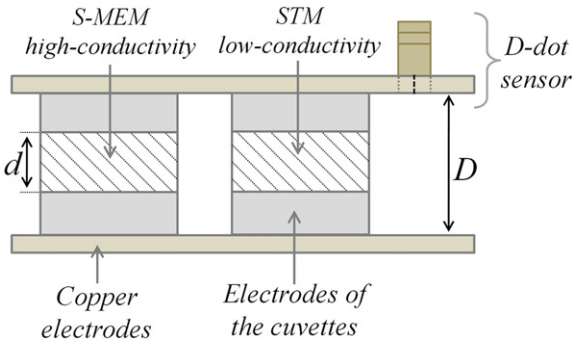

Fig. 2. Scheme of the experimental disposal.

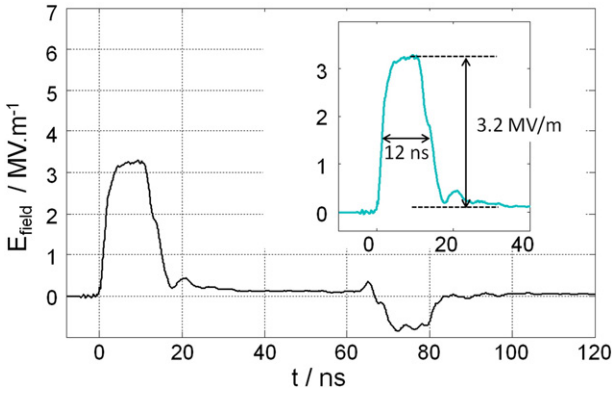

Fig. 3. Typical pulses applied in the experiments. The measurement displays the main pulse as well as the parasitic rebound. The main pulse characteristics are given in the inset.

applied to the two cuvettes. Polarization effects at the electrodes can be neglected, since they typically happen at very low frequencies (chapter 7 in [25]), while the high-frequency content of the 12-ns pulses is much higher [26]. Since cuvettes are filled with homogeneous medium, the electric field inside a cuvette is given by the voltage divided by the distance between the electrodes. The setup therefore ensures an identical electric field in the two media and the impact of conductivity can thus be evaluated.

The volume of cell suspension inside the cuvette was set to 400 µl. It was chosen in order to limit the reflection of the pulse at the level of the sample through the matching of the load impedance to the circuit and generator impedance. In order to prevent electrical breakdown in the air above the cell suspension, the remaining space between the electrodes was filled with paraffin oil (Sigma-Aldrich, Saint-Louis, MO, US).

Experiments designed to discriminate the impact of viscosity were performed with a generator from FID GmbH, Model FPG 10-ISM10. The 1 mm cuvettes from Molecular BioProducts were used (measured electrode distance d = 0.99 ± 0.08 mm) and the volume of cell suspension was 60 µl. A more precise description of the generator can be found in [13].

2.5. Nanosecond-pulsed electric field measurements

To perform experiments under controlled conditions, the electric field applied was measured systematically using a suitable sensor, namely, a D-dot that was directly attached to the exposure device [27]. Due to the position of the D-dot (displayed on Fig. 2), the field E_{D-dot} measured by the D-dot is the electric field between the two copper electrodes holding the cuvettes. The electric field E_{field} inside the cuvettes, which is considered to be the field strength applied to the cell sample, is computed according to (2), where d is the distance between the electrodes of the cuvette and D is the distance between the copper electrodes.

$$E_{field} = E_{D-dot}\frac{D}{d} \tag{2}$$

A typical pulse is represented in Fig. 3. The main pulse is trapezoidal with a duration at half-height of 12 ns and magnitude of 3.2 MV/m. It is followed by a negative rebound of approximately −0.8 MV/m, which is due to slight impedance mismatch.

2.6. Numerical methods

Transmembrane voltage V and the membrane's surface conductance were simulated using the model of DeBruin and Krassowska [28]. The cell is assumed to be spherical and embedded in the extracellular medium which is assumed to be infinite. The membrane voltage V can be approximated by Eq. (3), where S_0 is the initial surface conductance of the membrane, S_{ep} is the surface conductance of the permeabilized membrane given by Eq. (4), and N_{ep} is the pore density given by Eq. (5). The overall surface conductance of the membrane is thus $S = S_0 + S_{ep}$. The membrane voltage in the linear case, i.e. in the absence of permeabilization, is simply computed using Eq. (3) and considering that $S_{ep} = 0$. Note that in this case, the charging time of the membrane in the absence of permeabilization as mentioned in the Introduction (Eq. 1) can be computed easily using Eq. (3).

$$C_m\frac{\partial V}{\partial t} + \left(\frac{2\sigma_e\sigma_i}{r_c(\sigma_i+2\sigma_e)} + S_0 + S_{ep}(t,V)\right)V = \frac{3\sigma_e\sigma_i}{\sigma_i+2\sigma_e}E \tag{3}$$

$$S_{ep}(t,V) = S_1 N_{ep}(t,V) \tag{4}$$

$$\frac{\partial N_{ep}(t,V)}{\partial t} = \alpha e^{(V/V_{ep})^2}\left(1-\frac{N_{ep}}{N_0}\exp\left(-q(V/V_{ep})^2\right)\right) \tag{5}$$

The computational cost of the 3D model of DeBruin and Krassowska for 100 pulses is quite high. We therefore take advantage of the assumption of spherical cell shape and we use the expansion in Fourier modes to easily obtain preliminary results. The principal Fourier mode at the pole is computed. The time step equals 0.1 ns during pulse application. Note that between two pulses, V rapidly decreases to 0 (with a time constant of τ), such that pore density can be calculated explicitly without requiring a numerical solution with a small time step. The time step was thus set to 10 µs between the pulses. The parameters used for the simulation are given in Table 1.

The 3D model of Leguèbe et al. [17] was also used. The 3D code is based on finite difference methods in Cartesian grids, but once again we perform experiments using Fourier mode expansion. This model separates conductance increase and permeability increase. For a direct comparison with the model of DeBruin and Krassowska, only the conductance increase was computed. Eqs. (3) and (4) are still valid, while pore density is now given by Eq. (5'). Note that in the initial paper [17], pore density is described in a slightly different way, although the simulation results are largely identical. The parameters used for the

Table 1
Simulation parameters for the electropermeabilization model of Debruin and Krassowska. Except for the cell radius, the parameters are taken from [28].

r_c — cell radius	7 µm
σ_i — intra-cellular conductivity	1 S/m
S_0 — initial surface conductance of the membrane	1.9 S/m^2
C_m — membrane capacitance	0.01 F/m^2
V_{ep} — voltage threshold of electroporation	540 mV
N_0 — pore density at rest	$1.5 \cdot 10^9$ m^{-2}
q	2.46
α	10^9

Table 2
Simulation parameters for the electropermeabilization model of Lebègue et al. [17].

r_c — cell radius	7 μm
σ_i — intra-cellular conductivity	1 S/m
S_0 — initial surface conductance of the membrane	1.9 S/m^2
C_m — membrane capacitance	0.01 F/m^2
V_{ep} — voltage threshold of electroporation	1 V
S_1 — maximum surface conductance of the membrane	10^6 S/m^2
τ_{ep} — poration characteristic time	0.1 μs

simulations are given in Table 2.

$$\frac{\partial N_{ep}(t,V)}{\partial t} = \frac{1}{\tau_{ep}}\left(e^{-(V_{ep}/V)^2} - N_{ep}\right) \tag{5'}$$

3. Results

3.1. Efficiency of permeabilization

In order to determine the influence of conductivity on cell electropermeabilization, the cells were exposed to pulses of 12 ns in duration and 3.2 MV/m in magnitude. The repetition rate was chosen to be equal to 10 Hz, because a high number of pulses is required to observe biological effects [13]. 10 Hz ensured that the overall exposure time did not exceed 100 s. Experiments were performed simultaneously in the two media, as was described in the Material and methods section. Viability after the application of various numbers of pulses was tested using the cloning efficiency test. The results are presented in Fig. 4.

Without bleomycin, 500 pulses induced the death of 60% of the cells when they were exposed in the 1.5 S/m buffer (Fig. 4), while no mortality was induced by 1000 of these pulses in the 0.1 S/m buffer. When 30 nM of bleomycin was added to the extracellular medium, much less pulses were required to induce the same effects in the 1.5 S/m buffer. Merely 100 pulses were sufficient to induce 60% of cell death. In the 0.1 S/m buffer, however, no cell death was observed even after the application of 1000 pulses.

The results of Fig. 4 have been combined in order to discriminate the proportion of cells directly killed by the pulses from those that are killed in the presence of bleomycin only. The latter are considered to be 'reversibly permeabilized'. Those results are presented in Fig. 5. This figure illustrates that both direct killing and reversible permeabilization are observed in the 1.5 S/m buffer, whereas almost neither of them is observed in the 0.1 S/m buffer.

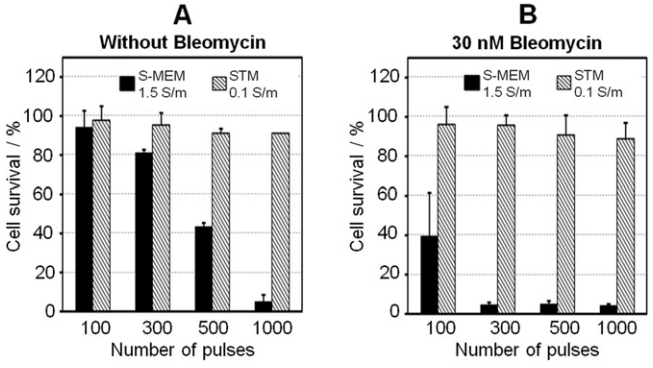

Fig. 4. Cell viability after exposure of cells to various numbers of pulses of 12 ns and 3.2 MV/m. The repetition rate was 10 Hz. Results are represented as mean values + SD (standard deviation) of three to five experiments. (A) Cells were exposed in medium alone. (B) Cells were exposed in medium containing 30 nM bleomycin. In B, cell survival is normalized to the control exposed to bleomycin alone.

3.2. Influence of temperature

The results presented above raise the question of the temperature increase of the samples. Indeed, if two media with different conductivities are exposed to the same electric field, a higher temperature increase is expected in the medium with the highest conductivity. In the above experiments, effects were observed in the high-conductivity medium only and could in principle be due to an increase of the medium temperature.

The maximum temperature increase can be estimated by a simple computation [29]. The approximate energy per volume $E_{dissipated}$ (expressed in J/m^3) dissipated through a sample due to N pulses can be calculated easily, if we approximate the pulses to square pulses of 12 ns and if only the resistive aspect of the media is considered. $E_{dissipated}$ is given by Eq. (6), where E is the local magnitude of the field (V/m), σ is the medium conductivity (S/m), and Δt is the duration of the pulse (s).

$$E_{dissipated} = \sigma \cdot |E|^2 \cdot \Delta t \cdot N \tag{6}$$

The temperature increase under adiabatic condition is then given by Eq. (7), where c_{water} is water-specific heat capacity ($c_{water} = 4.184$ J/(g·K) and d_{water} is the mass density of water ($d_{water} = 0.997 \times 10^6$ g/m^3).

$$\Delta T = \frac{\sigma \cdot |E|^2 \cdot \Delta t \cdot N}{c_{water} \cdot d_{water}} \tag{7}$$

The temperature increase computed for 100 pulses of 12 ns and 3.2 MV/m is approximately 4.4 °C which would heat up the medium from the room temperature of 22 °C to 26.4 °C. Such an increase is unlikely to permeabilize 60% of the cells to bleomycin (Fig. 4).

Moreover, if we consider that most of the energy is very rapidly transferred to the aluminum electrode (which is reasonable, since thermal transfer is very good between the water and the metal), then the temperature increase is given by Eq. (8), where c_{alu} is the aluminum's specific heat capacity ($c_{alu} = 0.897$ J/(g·K), d_{alu} is the mass density of aluminum ($d_{alu} = 2.7 \times 10^6$ g/m^3), V_{medium} is the volume of the cell suspension ($V_{medium} = 0.4$ cm^3), and V_{alu} is the volume of the electrodes ($V_{alu} = 0.64$ cm^3). In that case, the temperature increase caused by 100 pulses of 12 ns and 4.3 MV/m is approximately 2.3 °C.

$$\Delta T = \sigma \cdot |E|^2 \cdot \Delta t \cdot N \frac{V_{medium}}{(c_{alu} \cdot d_{alu} \cdot V_{alu} + c_{water} \cdot d_{water} \cdot V_{medium})} \tag{8}$$

Those rules-of-thumb computations consider that no energy is dissipated, which is, of course, the worst case. With a repetition rate of only 10 Hz, it is likely that part of the energy is dissipated while applying the pulse.

Since temperature measurement was not feasible without disturbing the experimental conditions, we decided to evaluate the temperature increase by means of electrical measurements. When several pulses are applied, all can be acquired using the pulse mode of the oscilloscope. For each pulse, the maximum of the field magnitude was extracted and plotted in Fig. 6A as a function of the pulse number in the sequence. As obvious from this figure, the pulse magnitude decreases slightly with time. Such a decrease corresponds to a slight heating of the sample. Indeed, it is known that heating increases the conductivity of saline solutions (-Chapter 2 in [25]). As a consequence, the overall conductivity of the sample will increase and, in turn, the magnitude of the applied electric pulse will change due to impedance mismatch. In this precise experiment, the sample consisted of two cuvettes with a 4 mm gap containing 400 μl of S-MEM or STM. Since the conductivity of S-MEM exceeds that of STM by more than a factor of ten, it will impose global impedance. Moreover, the conductance of the S-MEM medium imposes the magnitude of a 12-ns pulse [26]. The impedance of the sample can thus be approximated

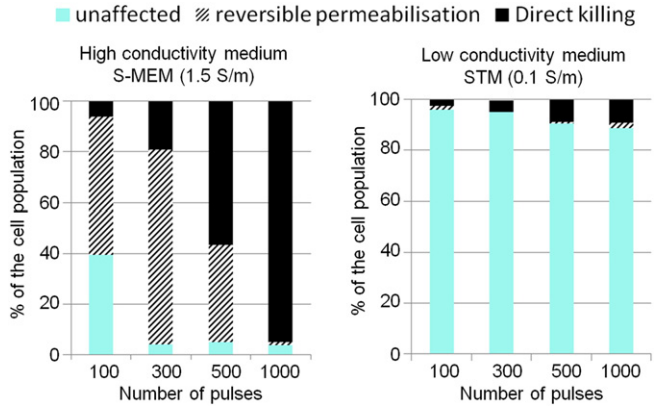

Fig. 5. Interpretation of the biological effects of the pulses for the two different media. Cells were exposed to a 12-ns pulse of 3.2 MV/m. The repetition rate is 10 Hz.

by Eq. (9), where S is the section through which the current flows and d is the distance between the electrodes.

$$Z = \frac{1}{\sigma_{S-MEM}} \cdot \frac{d}{S} \tag{9}$$

According to reflection rules, the magnitude of the applied electric field $E_{applied}$ can be written as a function of the voltage supplied by the generator V_g, of the impedance of the sample Z and of the characteristic impedance of the cable and the generator Z_c (10).

$$E_{applied} = \frac{V_{applied}}{d} = \frac{V_g}{d}\left(1 + \frac{Z - Z_c}{Z + Z_c}\right) \tag{10}$$

The conductivity of the sample is thus given by Eq. (11).

$$\sigma_{S-MEM} = \frac{d}{Z_c S}\left(\frac{2V_g}{V_{applied}} - 1\right) \tag{11}$$

The conductivity of S-MEM as a function of the temperature was evaluated in a separate experiment. The experimental data are presented in Fig. 6B. The data indicate that in this regime, the conductivity of the S-MEM is linear versus temperature. The conductivity can be approximated by Eq. (12), where $\alpha = 0.04\ S \cdot m^{-1} \cdot K^{1}$ and $\beta = 0.55\ S \cdot m^{-1}$.

$$\sigma = \alpha \cdot T + \beta \tag{12}$$

Hence, according to the three previous equations, temperature increase can be evaluated by Eq. (13).

$$T = \frac{1}{\alpha}\left[\frac{d}{Z_c S}\left(\frac{2V_g}{V_{applied}} - 1\right) - \beta\right] \tag{13}$$

In Fig. 6C, this expression is employed to compute the temperature as a function of the applied voltage. The temperature computed increases exponentially with time, which is coherent with a thermal increase. The initial temperature was estimated to be 23.8 °C which is

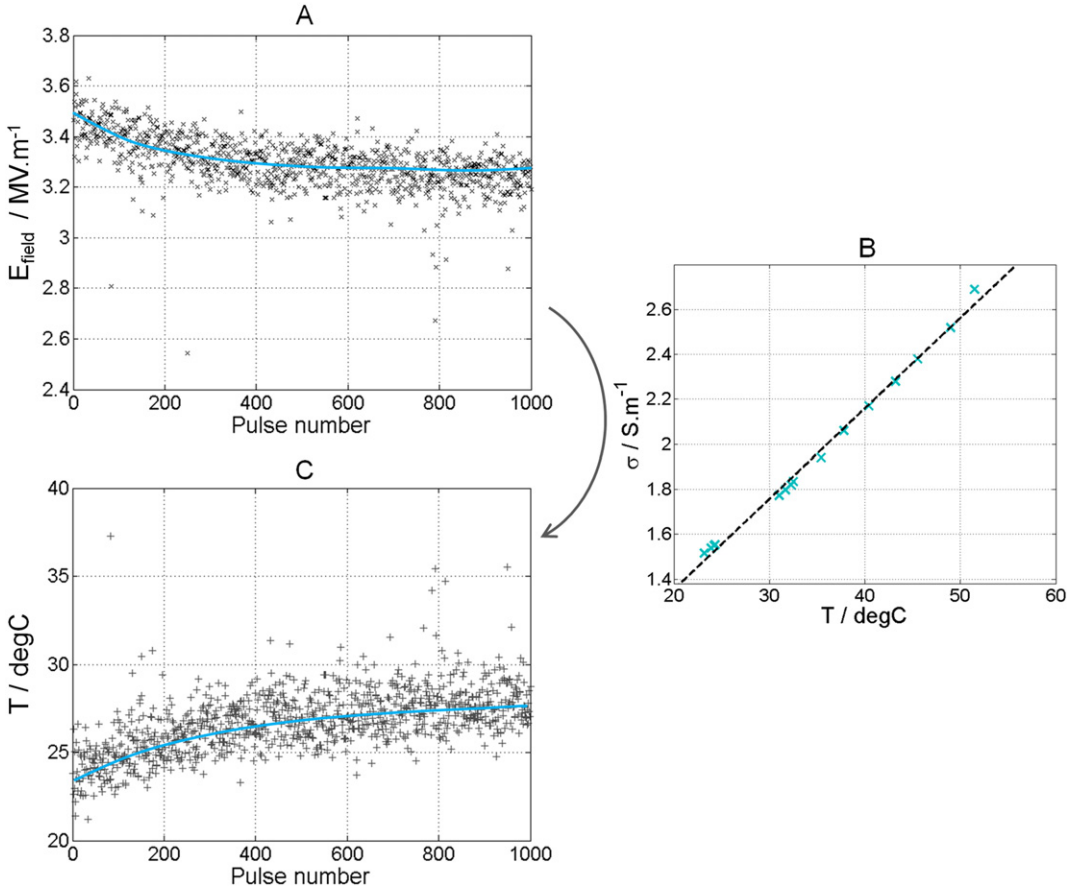

Fig. 6. (A) Measurement of the pulse magnitude as a function of the pulse number. (B) Conductivity of the S-MEM medium as a function of temperature. The graph displays individual data points and a linear regression in the form of $\sigma = \alpha \cdot T + \beta$ (parameters given in the text). (C) Temperature evaluated using pulse magnitude (see the text for more details).

also coherent with room temperature. After 100 pulses, the temperature increase is estimated to be around 1 or 2 °C, which is slightly lower than the 2.3 °C increase expected under adiabatic condition. Moreover, after 1000 pulses, the temperature is almost stabilized at its final value of 28 °C. A synergistic effect of electric pulses and temperature has already been described in the literature, but it requires a much higher temperature increase [30–34]. The slight temperature increase obtained during the experiments described above therefore cannot explain the huge permeabilization induced (Fig. 4).

3.3. Role of viscosity

Apart from having very different conductivities, the two media used in the experiments also have very different viscosities. The low-conductivity medium STM has a viscosity of $1.06 \pm 0.07 \cdot 10^{-2}$ P which is significantly higher than that of the high-conductivity medium S-MEM, which is $0.89 \pm 0.03 \cdot 10^{-2}$ P. This is due to the large amount of sucrose contained in STM. In order to account for the role viscosity might play, 0.1% or 0.15% agar was added to the high-conductivity medium in order to modify its viscosity. The conductivity was not changed by the addition of agar. Over 0.15% of agar, the high viscosity prevented the cuvette from being filled with the exactly pre-defined volume, which led to pulse distortion. The high viscosity also caused important biases in cell collection and, hence, in colony counts. The viscosity values for the S-MEM medium containing 0.1% and 0.15% agar were $5.6 \cdot 10^{-2}$ P and $61 \cdot 10^{-2}$ P, respectively. Fig. 7 shows the result of cloning efficacy experiments performed with different percentages of agar in the medium. The treatment consisted in the application of 500 pulses of 10 ns duration and a field magnitude of 4.2 MV/m (note that the generator was different). The repetition rate was kept at 10 Hz. Under those conditions, viscosity did not appear to be a key parameter, as the percentage of clones was the same with all media.

4. Discussion

Several groups studied the influence of conductivity on the efficiency of conventional permeabilization by pulses of microseconds or milliseconds in duration [2,35–37]. In most cases, those studies indicate that a decrease in extracellular medium conductivity slightly decreases the efficiency of the permeabilization [38]. However, this influence is very weak and can only be observed for very low values of conductivity, typically less than 0.01 S/m [38].

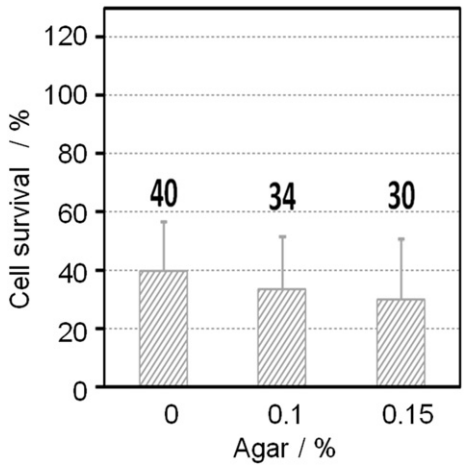

Fig. 7. Viability based on the viscosity of the medium. 500 pulses of magnitude 4.2 MV/m and length of 10 ns were applied with a repetition rate of 10 Hz. The extracellular medium was S-MEM, eventually supplemented with agar. The results are the average ± SD of 3 experiments (generator from FID GmbH, Model FPG 10-ISM10 and 1 mm cuvettes from Molecular BioProducts were used). For each agar concentration, results were normalized to the control which consisted in unpulsed cells in the same medium, with the same agar concentration and with 30 nM bleomycin.

An influence of conductivity for short pulses has already been suggested in a theoretical study, where the authors proposed that permeabilization by nanosecond pulses should be scaled by the charge density. According to this hypothesis, permeabilization is supposed to be more efficient in high-conductivity media [39]. The only experimental work in which this question was addressed, however, reveals a higher efficiency of the low-conductivity media [9]. The results obtained here show the opposite dependence on conductivity. With the 12-ns pulses used here, more cell death and more reversible permeabilization were induced in the DC-3F cells in the high-conductivity medium. Under the conditions of our experiments, thermal effects were found to be negligible. Moreover, the viscosity of the extracellular media did not have any influence. Electrochemical reactions at the electrode interface could play a role in the observed results. Indeed, it is well known that some of the chemical species formed can affect biological cells and even lead to cell death (a phenomenon which is used in the electrochemical treatment of tumors [40]). The importance of the phenomenon will depend on the chemical composition of the medium as well as on the type of metal used for the electrodes. Since the number of chemical species created is proportional to the charge injected, the dose used to quantify electrochemical reaction generally is the number of charges to volume Q_v (C/m^3) which can be evaluated according to formula (14) [29].

$$Q_v = \frac{\sigma \cdot |E| \cdot \Delta t \cdot N}{d} \tag{14}$$

Under the worst conditions tested, when 1000 pulses were applied, we obtained a charge per volume of 1.4×10^4 C/m^3 in the high-conductivity medium in which cell death and permeabilization were observed. This value is approximately 20 times lower than the threshold of 3×10^5 C/m^3 reported in the paper of Yen and colleagues to observe an impact of electrochemically generated species on cell growth [41]. Potential influence of electrochemical reactions, however, cannot be ruled out completely, since the studies have only been carried out with an electric field of low magnitude. At higher electric fields, electrochemical reactions might be modified as well as their kinetics. Lower doses than the one mentioned by Yen [41] might thus be sufficient to induce some biological consequences. However, we believe that the influence of electrochemical reactions is probably limited, since cells are kept in the pulsing buffer only for 10 min, while it is generally admitted that cells should be kept in the presence of the toxic chemical species for a longer time in order to observe a deleterious effect [41,42]. Moreover, not only cell death has been observed, but also reversible electropermeabilization as assessed by the uptake of bleomycin. To our knowledge, no studies suggest that electrochemical reactions can induce a reversible permeabilization of cell membrane.

Since effects of temperature, viscosity, and chemical reactions can be excluded, the observed impact of conductivity is likely to be of an electrical nature. At first glance, the fact that the high-conductivity medium is more efficient for cell electroporation seems to be intuitive from an electrical point of view. It might be reasoned that the membrane voltage reaches a higher value in the higher-conductivity medium, since charging time is shorter than in the low-conductivity medium and cells are not fully charged by the end of the pulse in both cases, since pulse duration is smaller than charging time in the two cases. This is typically what linear electromagnetic models describe. The theoretical transmembrane voltages (TMVs) induced by the external electric field across the membrane of cells are displayed in Fig. 8. Only induced TMV is represented and the possible contribution of the resting TMV is neglected. Taking resting TMV into account, however, would not change the interpretation of the following simulations. Only the value at the cell's poles has been represented ($\theta = 0$ or $\theta = \pi$, see inset in the figure). These results

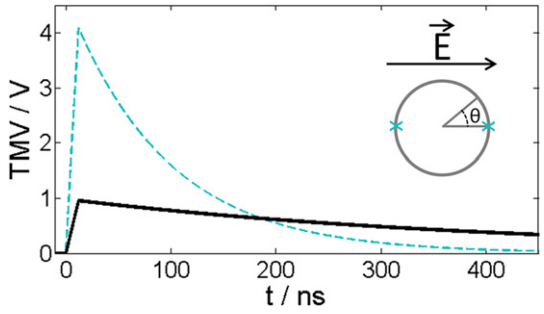

Fig. 8. Simulation of the transmembrane voltages during a 12-ns pulse of 3.2 MV/m and in the linear case. The displayed values correspond to what is expected at the pole of the cell, for $\theta = 0[\pi]$ as depicted in the inset. The dotted blue line corresponds to S-MEM ($\sigma_e = 1.5\ S.m^{-1}$) and the solid black line to STM ($\sigma_e = 0.1\ S.m^{-1}$).

were obtained using strictly linear models, which implies that no change in the properties of the membrane is taken into account. In particular, a potential increase of membrane conductivity during the pulse due to electroporation is not accounted for (see Material and methods). For both extracellular media, we observe that the induced transmembrane voltage increases continuously during the pulse, while it relaxes back to 0 mV when the electric field is switched off. The fact that the TMV increases continuously is coherent with the fact that the pulse duration is smaller than the charging times of the membrane in both media, which, according to the model, are equal to $\tau_1 = 93$ ns in the high-conductivity medium and $\tau_2 = 420$ ns in the low-conductivity medium. Since charging time in the high-conductivity medium is shorter than that in the low-conductivity medium, the TMV reaches a much higher value at the end of the pulse. Theoretically, approximately 4 V can be achieved in the high-conductivity medium, while the TMV barely exceeds 1 V in the low-conductivity medium. As mentioned before, the model used to compute the TMV is linear and does not take into account the eventual feedback the permeabilization of the membrane might have on the value of the TMV. It is legitimate to assume, however, that the TMV will reach higher values in the more conductive medium, which could provide an explanation for the difference in permeabilization efficiency that was observed in the experiments.

Standard electroporation models which account for membrane conductance increase like the one of DeBruin and Krassowska [28] also suggest that the high-conductivity medium should be more efficient. The values of the transmembrane voltage (at the pole) as well as the overall surface conductance of the membrane computed according to this model are displayed in Fig. 9A. In the case of the low-conductivity medium, surface conductance of the membrane does not increase and the transmembrane voltage is identical to that obtained in the linear case. In the high-conductivity medium, however, conductance of the membrane increases, which affects the transmembrane voltage by slightly accelerating the discharge after the pulse. Nevertheless, the qualitative behavior the TMV is very close to that obtained in the linear case. Similar results for the transmembrane voltage and surface conductance of the membrane are obtained with the electric part of the model of Leguèbe et al. [17], as displayed in Fig. 9B. Note that the main difference to the previous model is that the surface conductance of the membrane increases more slowly when permeabilization starts. Both models include a number of unknown parameters, such as intracellular conductivity or the membrane's initial surface conductance. Changing the values of these parameters will, of course, influence the outcome of the simulation and the exact values of TMV or membrane surface conductance. However, both models always yield results which are qualitatively identical to those displayed in Fig. 9.

We emphasize that the above computational results are valid for one pulse only, while the experiments were conducted with hundreds or even a thousand pulses. In Fig. 10A we plot the membrane TMV and the membrane surface conductance after 10 pulses using the model of Debruin and Krassowska. In such a model each pulse generates the same transmembrane voltage. The conductance of the membrane reaches its highest value after the first pulse and progressively decreases. Since one of the postulates of this model is that the intensity of permeabilization is reflected by the value of membrane conductance, this model suggests that cumulating pulses will not increase the impact of the treatment. Indeed, subsequent pulses do not increase the conductance of the membrane more than the first pulse does. Similar results are obtained when cumulating more than 10 pulses (results not shown). This important drawback is due to the fact that the transmembrane voltage has a "local" effect. Since no diffusion of the membrane defects (pores in the case of this model) is accounted for, the induced TMV is always established on the same fraction of the membrane which is permeabilized by the first pulse. The model of

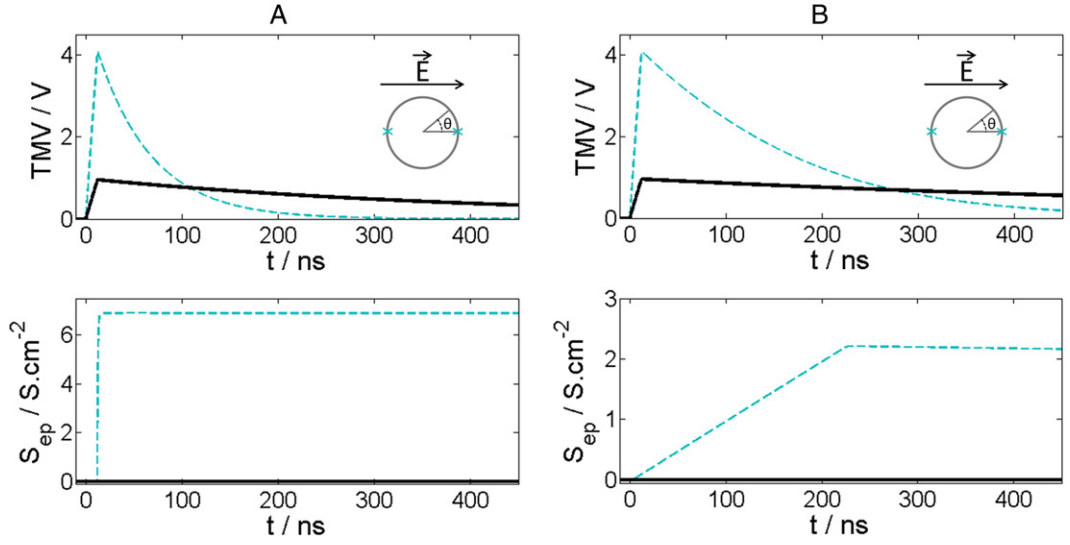

Fig. 9. Simulation of the transmembrane voltage and membrane surface conductance during a 12-ns pulse of 3.2 MV/m. Panel (A) shows the model of Debruin and Krassowska and panel (B) the model of Leguèbe et al. The displayed values of the transmembrane voltage and surface conductance correspond to what is expected at the pole of the cell, for $\theta = 0[\pi]$ as depicted in the inset. The dotted blue line corresponds to S-MEM ($\sigma_e = 1.5\ S.m^{-1}$) and the solid black line to STM ($\sigma_e = 0.1\ S.m^{-1}$).

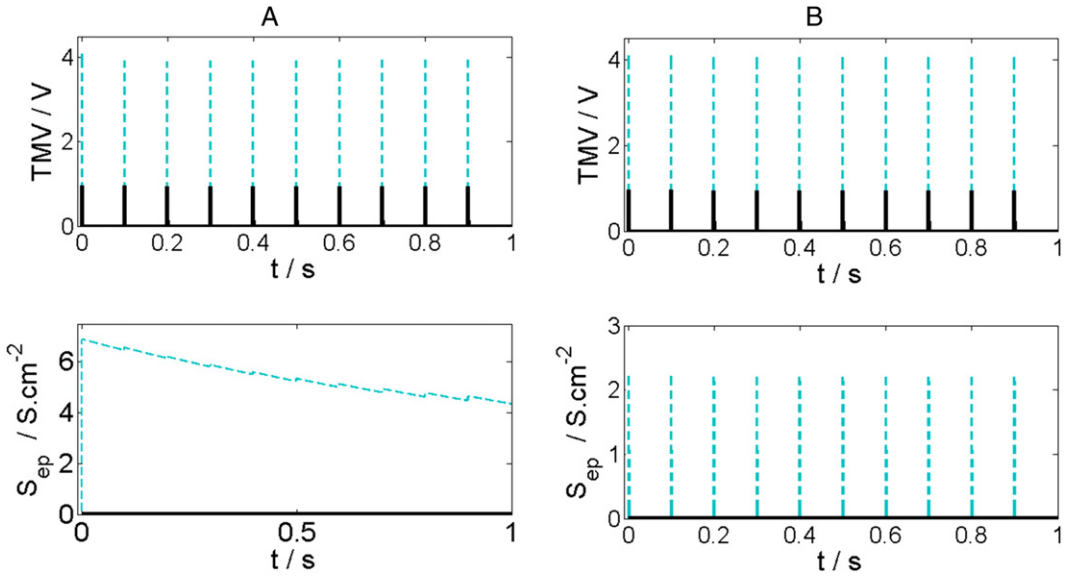

Fig. 10. Simulation of the transmembrane voltage and membrane surface conductance during a sequence of 10 pulses of 12 ns and 3.2 MV/m applied with a repetition rate of 10 Hz. Panel (A) corresponds to the model of Debruin and Krassowska and panel (B) to the model of Leguèbe et al. The displayed values of the transmembrane voltage and surface conductance correspond to what is expected at the pole of the cell, for $\theta = 0[\pi]$ as depicted in Figs. 8 and 9. The dotted blue line corresponds to S-MEM ($\sigma_e = 1.5\ S \cdot m^{-1}$) and solid black line to STM ($\sigma_e = 0.1\ S \cdot m^{-1}$).

Leguèbe et al. [17] that does not have this drawback can therefore better describe the results and especially the effect of pulse accumulation. First, the model separates conductance and permeability. Conductance increase is thought to be due to some pore creation (like in the model of Debruin and Krassowska). However, pores are considered to rapidly collapse so that the membrane rapidly recovers a conductance equal or close to the initial conductance. This implies that in a series of pulses, each pulse can generate a high transmembrane voltage on the membrane, since the conductance of the membrane has recovered. This is typically what can be seen in Fig. 10B which is the simulation for 10 consecutive pulses applied at 10 Hz. Each pulse has merely the same impact on the conductance of the membrane. The fact that pulses have a cumulative effect on membrane permeability therefore is not observed for membrane conductance. However, when looking at the permeability of the membrane, such an effect is visible, as was shown by simulations in the paper presenting the model [17]. At this current stage, the model cannot give any precise physical interpretation of the permeability. However, more permanent change in the physical or chemical properties of the lipids may be initiated by the pores. Moreover, since the model considers that the 'defects' or 'local change of membrane properties' can diffuse away from the pole regions, where they were initially generated, new defects can be generated by subsequent pulses. This diffusion process of defects is thus essential to describe the effect of pulse repetition as well as the influence of the pulse repetition rate.

5. Conclusion

The experiments presented in this paper illustrate that mammalian cells can be permeabilized efficiently by 12-ns electric pulses. With the electrical parameters used – 12 ns and 3.2 MV/m –, a major influence of the conductivity of the external medium was observed. The most conductive medium (1.5 S/m) induced both efficient reversible permeabilization and efficient direct killing of the cells. In contrast to this, the same number of pulses induced hardly any effect when the conductivity of the external medium was reduced to 0.1 S/m. We have shown that this difference was neither a thermal artifact nor a consequence of a difference of viscosity between the two media. The probability of occurrence of an electrochemical artifact was estimated to be negligible. We are therefore confident that the observed difference is a true electrical phenomenon. According to the classical electromagnetic models of cells, charging time of cell membrane is highly influenced by the conductivity of the external medium. Membrane charging happens faster when the external medium has a higher conductivity. For an electric pulse shorter than the charging time of the membrane, as it was the case under our working conditions, the voltage induced across cell membrane can in principle reach higher values when the external medium has a higher conductivity. We believe that this is the most probable explanation of the results observed. This remains to be confirmed experimentally by measurements of the transmembrane voltage using fluorescence voltage reporters, for instance. Proving the validity of this hypothesis is essential for our understanding of interactions of short electric pulses with biological cells. It has not yet been determined whether the impact of short pulses on biological cells is a conductive or a purely dielectric effect. The influence of conductivity found here supports the fact that charges still play a role, even with 12-ns pulses. Finally, it should be noted that the influence of the type of ions and, in particular, the impact of their mobility has not yet been investigated. This will be an important step towards understanding the impact of pulsed electric field on biological cells.

Conflict of interest

The authors have no conflict of interest with respect to this research article.

Author contributions

Conception and design of the study: AS, IL, and LM. Acquisition of data: AS and IL. Simulations: ML and CP. Interpretation of data: All authors. Drafting and critical revising of the manuscript: AS, CP, and LM. Additionally, all authors approved of the final version of the manuscript to be submitted.

Acknowledgments

The authors were funded partly by the French National Agency under the research project MEMOVE (2011-BS01-006-01). Part of this

work was performed in the International Associated Laboratory EBAM. The work of C.P. and M.L. was carried out with financial support by the state of France via the French National Research Agency (ANR) within the framework of the "Investments for the future" Program IdEx Bordeaux-CPU (ANR-10-IDEX-03-02). The work was also supported by CNRS, University Paris-Sud, Gustave Roussy, and the Fondation EDF.

Numerical results presented in this paper were obtained using the PLAFRIM numerical test bed developed under the Inria PlaFRIM development action with support from LABRI and IMB and other institutions: Conseil Régional d'Aquitaine, FeDER, Université de Bordeaux, and CNRS (see https://plafrim.bordeaux.inria.fr/).

The authors would like to thank Marie-Amélie de Ménorval for providing the viscosity measurements and Lars H. Wegner for the critical reading of the manuscript. The authors also acknowledge valuable discussions on basic mechanisms within the framework of COST TD1104.

References

[1] L.M. Mir, H. Banoun, C. Paoletti, Introduction of definite amounts of nonpermeant molecules into living cells after electropermeabilization: Direct access to the cytosol, Exp. Cell Res. 175 (1988) 15–25, http://dx.doi.org/10.1016/0014-4827(88)90251-0.

[2] E. Neumann, Membrane electroporation and direct gene transfer, Bioelectrochem. Bioenerg. 28 (1992) 247–267, http://dx.doi.org/10.1016/0302-4598(92)80017-B.

[3] J. Teissie, M. Golzio, M.P. Rols, Mechanisms of cell membrane electropermeabilization: a minireview of our present (lack of ?) knowledge, Biochim. Biophys. Acta 1724 (2005) 270–280, http://dx.doi.org/10.1016/j.bbagen.2005.05.006.

[4] L.M. Mir, Bases and rationale of the electrochemotherapy, Eur. J. Cancer Suppl. 4 (2006) 38–44, http://dx.doi.org/10.1016/j.ejcsup.2006.08.005.

[5] A. Silve, L.M. Mir, Cell Electropermeabilization and Cellular Uptake of Small Molecules: The Electrochemotherapy Concept, in: S.T. Kee, J. Gehl, E.W. Lee (Eds.), Clin. Asp. Electroporation, Springer, New York, NY 2011, pp. 69–82 http://www.springerlink.com.gate1.inist.fr/content/r86178281342200g/ (accessed July 29, 2011).

[6] M. Breton, L.M. Mir, Microsecond and Nanosecond Electric Pulses in Cancer Treatments, Bioelectromagnetics, 2011. http://dx.doi.org/10.1002/bem.20692.

[7] C. Jiang, R.V. Davalos, J.C. Bischof, A review of basic to clinical studies of irreversible electroporation therapy, I.E.E.E. Trans. Biomed. Eng. 62 (2015) 4–20, http://dx.doi.org/10.1109/TBME.2014.2367543.

[8] R. Nuccitelli, R. Wood, M. Kreis, B. Athos, J. Huynh, K. Lui, et al., First-in-human trial of nanoelectroablation therapy for basal cell carcinoma: proof of method, Exp. Dermatol. 23 (2014) 135–137, http://dx.doi.org/10.1111/exd.12303.

[9] K.J. Müller, V.L. Sukhorukov, U. Zimmermann, Reversible electropermeabilization of mammalian cells by high-intensity, ultra-short pulses of submicrosecond duration, J. Membr. Biol. 184 (2001) 161–170.

[10] A.G. Pakhomov, J.F. Kolb, J.A. White, R.P. Joshi, S. Xiao, K.H. Schoenbach, Long-lasting plasma membrane permeabilization in mammalian cells by nanosecond pulsed electric field (nsPEF), Bioelectromagnetics 28 (2007) 655–663, http://dx.doi.org/10.1002/bem.20354.

[11] O.M. Nesin, O.N. Pakhomova, S. Xiao, A.G. Pakhomov, Manipulation of cell volume and membrane pore comparison following single cell permeabilization with 60- and 600-ns electric pulses, Biochim. Biophys. Acta 1808 (2011) 792–801, http://dx.doi.org/10.1016/j.bbamem.2010.12.012.

[12] P.T. Vernier, Y. Sun, M.A. Gundersen, Nanoelectropulse-driven membrane perturbation and small molecule permeabilization, BMC Cell Biol. 7 (2006) 37, http://dx.doi.org/10.1186/1471-2121-7-37.

[13] A. Silve, I. Leray, L.M. Mir, Demonstration of cell membrane permeabilization to medium-sized molecules caused by a single 10ns electric pulse, Bioelectrochemistry (2011)http://dx.doi.org/10.1016/j.bioelechem.2011.10.002 (Amst. Neth).

[14] H. Pauly, H. Schwan, Uber die impedanz einer suspension von kugelförmigen teilchen mit einer schale, Z. Naturforsch. 14B (1959) 125–131.

[15] T. Kotnik, D. Miklavcic, Second-order model of membrane electric field induced by alternating external electric fields, Biomed. Eng. IEEE Trans. On. 47 (2000) 1074–1081, http://dx.doi.org/10.1109/10.855935.

[16] O. Kavian, M. Leguèbe, C. Poignard, L. Weynans, "Classical" Electropermeabilization Modeling at the Cell Scale, J. Math. Biol. 68 (1–2) (2014) 235–265, http://dx.doi.org/10.1007/s00285-012-0629-3.

[17] M. Leguèbe, A. Silve, L.M. Mir, C. Poignard, Conducting and permeable states of cell membrane submitted to high voltage pulses: mathematical and numerical studies validated by the experiments, J. Theor. Biol. 360C (2014) 83–94, http://dx.doi.org/10.1016/j.jtbi.2014.06.027.

[18] B. Poddevin, S. Orlowski, J. Belehradek Jr., L.M. Mir, Very high cytotoxicity of bleomycin introduced into the cytosol of cells in culture, Biochem. Pharmacol. 42 (1991) S67–S75 Suppl.

[19] G. Pron, J. Belehradek Jr., L.M. Mir, Identification of a plasma membrane protein that specifically binds bleomycin, Biochem. Biophys. Res. Commun. 194 (1993) 333–337, http://dx.doi.org/10.1006/bbrc.1993.1824.

[20] G. Pron, J. Belehradek Jr., S. Orlowski, L.M. Mir, Involvement of membrane bleomycin-binding sites in bleomycin cytotoxicity, Biochem. Pharmacol. 48 (1994) 301–310.

[21] G. Pron, N. Mahrour, S. Orlowski, O. Tounekti, B. Poddevin, J. Belehradek Jr., et al., Internalisation of the bleomycin molecules responsible for bleomycin toxicity: a receptor-mediated endocytosis mechanism, Biochem. Pharmacol. 57 (1999) 45–56.

[22] O. Tounekti, G. Pron, J. Belehradek Jr., L.M. Mir, Bleomycin, an apoptosis-mimetic drug that induces two types of cell death depending on the number of molecules internalized, Cancer Res. 53 (1993) 5462–5469.

[23] T. Kotnik, A. Macek-Lebar, D. Miklavcic, L.M. Mir, Evaluation of cell membrane electropermeabilization by means of a nonpermeant cytotoxic agent, Biotechniques 28 (2000) 921–926.

[24] J.L. Biedler, H. Riehm, Cellular resistance to actinomycin D in Chinese hamster cells in vitro: cross-resistance, radioautographic, and cytogenetic studies, Cancer Res. 30 (1970) 1174–1184.

[25] S. Grimnes, Ø.G. Martinsen, Bioimpedance and Bioelectricity Basics, Academic Press, 2008.

[26] A. Silve, R. Vézinet, L.M. Mir, Nanosecond-duration electric pulse delivery in vitro and in vivo: experimental considerations, Instrum. Meas. IEEE Trans. On. PP (2012) 1–10, http://dx.doi.org/10.1109/TIM.2012.2182861.

[27] A. Silve, R. Vezinet, L.M. Mir, Implementation of a Broad Band, High Level Electric Field Sensor in Biological Exposure Device, 2010. 711–714, http://dx.doi.org/10.1109/IPMHVC.2010.5958458.

[28] K.A. DeBruin, W. Krassowska, Modeling electroporation in a single cell. I. Effects of field strength and rest potential, Biophys. J. 77 (1999) 1213–1224.

[29] A. Silve, J. Villemejane, V. Joubert, A. Ivorra, L.M. Mir, Chapter 18 in Advanced Electroporation Techniques in Biology and Medicine, CRC Press, 2010.

[30] J.E. Dunn, J.S. Pearlman, Methods and Apparatus for Extending the Shelf Life of Fluid Food Products, US4695472 A, 1987. http://www.google.com/patents/US4695472 (accessed September 12, 2014).

[31] M.I. Bazhal, M.O. Ngadi, G.S.V. Raghavan, J.P. Smith, Inactivation of *Escherichia coli* O157:H7 in liquid whole egg using combined pulsed electric field and thermal treatments, LWT Food Sci. Technol. 39 (2006) 420–426, http://dx.doi.org/10.1016/j.lwt.2005.02.013.

[32] M. Amiali, M.O. Ngadi, J.P. Smith, G.S.V. Raghavan, Synergistic effect of temperature and pulsed electric field on inactivation of *Escherichia coli* O157:H7 and *Salmonella enteritidis* in liquid egg yolk, J. Food Eng. 79 (2007) 689–694, http://dx.doi.org/10.1016/j.jfoodeng.2006.02.029.

[33] H. El Zakhem, J.-L. Lanoiselle, N.I. Lebovka, M. Nonus, E. Vorobiev, Influence of temperature and surfactant on *Escherichia coli* inactivation in aqueous suspensions treated by moderate pulsed electric fields, Int. J. Food Microbiol. 120 (2007) 259–265, http://dx.doi.org/10.1016/j.ijfoodmicro.2007.09.002.

[34] J.T. Camp, Y. Jing, J. Zhuang, J.F. Kolb, S.J. Beebe, J. Song, et al., Cell death induced by subnanosecond pulsed electric fields at elevated temperatures, IEEE Trans. Plasma Sci. 40 (2012) 2334–2347, http://dx.doi.org/10.1109/TPS.2012.2208202.

[35] V.L. Sukhorukov, H. Mussauer, U. Zimmermann, The effect of electrical deformation forces on the electropermeabilization of erythrocyte membranes in low- and high-conductivity media, J. Membr. Biol. 163 (1998) 235–245.

[36] G. Pucihar, T. Kotnik, M. Kanduser, D. Miklavcic, The influence of medium conductivity on electropermeabilization and survival of cells in vitro, Bioelectrochemistry Amst. Neth. 54 (2001) 107–115.

[37] E. Ferreira, E. Potier, D. Logeart-Avramoglou, S. Salomskaite-Davalgiene, L.M. Mir, H. Petite, Optimization of a gene electrotransfer method for mesenchymal stem cell transfection, Gene Ther. 15 (2008) 537–544, http://dx.doi.org/10.1038/gt.2008.9.

[38] A. Ivorra, J. Villemejane, L.M. Mir, Electrical modeling of the influence of medium conductivity on electroporation, Phys. Chem. Chem. Phys. 12 (2010) 10055, http://dx.doi.org/10.1039/c004419a.

[39] K. Schoenbach, R. Joshi, S. Beebe, C. Baum, A scaling law for membrane permeabilization with nanopulses, IEEE Trans. Dielectr. Electr. Insul. 16 (2009) 1224–1235, http://dx.doi.org/10.1109/TDEI.2009.5293932.

[40] E. Nilsson, H. von Euler, J. Berendson, A. Thörne, P. Wersäll, I. Näslund, et al., Electrochemical treatment of tumours, Bioelectrochemistry 51 (2000) 1–11, http://dx.doi.org/10.1016/S0302-4598(99)00073-2.

[41] Y. Yen, J.R. Li, B.S. Zhou, F. Rojas, J. Yu, C.K. Chou, Electrochemical treatment of human KB cells in vitro, Bioelectromagnetics 20 (1999) 34–41.

[42] R. Rodaite-Riseviciene, R. Saule, V. Snitka, G. Saulis, Release of iron ions from the stainless steel anode occurring during high-voltage pulses and its consequences for cell electroporation technology, IEEE Trans. Plasma Sci. 42 (2014) 249–254, http://dx.doi.org/10.1109/TPS.2013.2287499.

Aude Silve was born in France in 1983. She received her M.S. degree in physics and biology interactions from the University of Paris 11, France. She then obtained her Ph.D. degree at the UMR 8203 CNRS-Institute Gustave-Roussy, Villejuif, France under the supervision of Lluis M. Mir. Since 2012, she has been working as a post-doc at the Institute for Pulsed Power and Microwave Technology of Karlsruhe Institute of Technology, Germany. Her current research interests include effects of nanosecond duration pulses on living cells and studies of transmembrane voltage and voltage-sensitive dyes.

Isabelle Leray was born in France in 1982. She received her M.S. degree in Applied Molecular Cytology from the University of Montpellier II, France. She is currently an assistant engineer at the UMR 8203 CNRS-Institute Gustave-Roussy, Villejuif, France. Her current research interests focus on effects of microsecond and nanosecond duration pulses on living cells.

Michael Leguèbe was born in 1984 in France. He received his PhD degree in Applied Mathematics from the University of Bordeaux, France. He is currently a post-doctoral scientist at the Max Planck Institute for Solar System Research in Göttingen, Germany. His current research interests include mathematical modeling and derivation of methods to solve partial differential equations.

Clair Poignard was born in 1979 in Saint Lô, France. He received the M.S. degree in Applied Mathematics from ENS Cachan-Bretagne and Université Rennes I, France, in 2003, and the Ph.D. degree from Université Lyon1, France, in 2006. He is currently working as a research scientist at INRIA Bordeaux-Sud Ouest, France. His main interests lie in the mathematical modeling of biological phenomena.

Lluis M. Mir from Ecole Normale Supérieure, Paris obtained his Ph.D in Toulouse. He is the Director of the Laboratory of Vectorology and Anticancer Therapies (UMR 8203 CNRS-University Paris-Saclay at Gustave Roussy, Villejuif, France). In 2010, he founded the European Associated Laboratory for the Applications of Electric Pulses in Biology and Medicine that he will co-direct until 2018. He published 196 scientific articles and 21 book chapters (H index = 57). His main interests lie in the fields of membrane electropermeabilization. He conceived and developed electrochemotherapy and also made seminal contributions to the electrotransfer of genes.